Thermal diffuse scattering from colloidal crystals

Paul A. Rundquist, R. Kesavamoorthy,[a] S. Jagannathan, and Sanford A. Asher[b]
University of Pittsburgh, Department of Chemistry, Pittsburgh, Pennsylvania 15260

(Received 30 January 1991; accepted 3 April 1991)

Measurement of the Bragg diffraction and thermal diffuse scattering from colloidal crystals consisting of aqueous suspensions of polystyrene spheres with and without strongly absorbing dye molecules show that dynamical diffraction theory is valid even for absorbing colloidal crystals. In addition, we show that thermal diffuse scattering from colloidal crystals may be described by the simple Debye model. We determine the effective penetration depth of the incident electric field for cases where the Bragg condition is satisfied.

INTRODUCTION

Colloidal crystals form spontaneously from deionized aqueous suspensions of charged monodisperse polystyrene spheres.[1-3] The surface charge on the colloidal spheres derives from the dissociation of strong acid (either sulfate or sulfonate) groups which are incorporated during the sphere synthesis. Because the dominant interparticle interaction is a screened Coulomb repulsion, the colloidal spheres spontaneously adopt a three dimensionally ordered crystal structure to minimize the repulsive interparticle interactions. The crystal structure of the lattice is determined by parameters such as the particle number density, the number of surface charge groups per sphere, the suspension ionic strength, and the particle diameter.[1-5] Large three dimensionally ordered colloidal crystals efficiently Bragg diffract light;[5-8] this property has recently been exploited to develop novel narrow-band optical rejection filters for use in optics and Raman spectroscopy.[8-10]

In addition, colloidal crystals, similar to atomic crystals, exhibit collective lattice vibrations. Hurd *et al.*[11,12] pioneered the study of colloidal crystal phonons. They measured the phonon dispersion curves and showed that these lattice vibrations are, in general, strongly damped. The lattice dynamics of colloidal crystals affect the diffraction phenomena. We previously showed that the dynamical diffraction theory origially proposed for x-ray diffraction may be used to model bandwidths and intensities for light diffraction by colloidal crystals;[5] in the present work we use dynamical diffraction theory to determine phonon scattering.

We measure the diffracted intensity as a function of incident angle at different solid angles of diffracted light for colloidal crystals prepared from aqueous suspensions of strongly absorbing (dyed) and nonabsorbing (undyed) polystyrene spheres. We find that the measured diffracted intensity increases with increasing acceptance solid angle, and that most of this intensity increase results from inelastic scattering of the incident light by crystal lattice vibrations. We show that the theory for thermal diffuse scattering (TDS) of x rays from atomic crystals is also valid for TDS from colloidal crystals. We determine the effective penetration depth of the incident electric field into the colloidal crystals from the TDS intensity distribution when the Bragg diffraction condition is satisfied.

EXPERIMENT

The synthetic procedure used to prepare the 83 nm ($+/-5\%$) diameter sulfonated polystyrene spheres will be presented elsewhere. An aliquot of aqueous sphere suspension was dyed[13] with Oil Red O (Aldrich), a nonfluorescing dye which strongly absorbs 515 nm light. The dyed and undyed spheres used to make the large colloidal crystals were dialyzed against high purity water for two weeks. The particle diameter was determined by quasielastic light scattering (QELS) and was verified by transmission electron microscopy (TEM). The surface charge number per sphere was determined to be 2370 ± 80 by measuring the suspension conductivity as a function of the volume fraction of polystyrene.[14] The volume fraction of polystyrene was determined from the suspension refractive index,[5] which was measured with a temperature controlled Abbe' refractometer.

Large single colloidal crystals of dyed and undyed 83 nm diam polystyrene spheres were prepared according to previously published techniques.[9,10] The cleaned deionized colloidal suspensions were injected into cells consisting of two quartz plates separated by a 0.05 cm thick spacer. The colloidal crystals were allowed to anneal for ca. one week. The dimensions of the cells holding the crystals were $2.5 \times 2.5 \times 0.05$ cm. Both crystals showed the Kossel ring pattern of a twinned body-centered-cubic (bcc) lattice where the (110) planes are parallel to the cell plates.[5]

The experimental diffraction geometry was similar to that previously reported.[5] The vertically polarized 514.5 nm line of a Spectra Physics model 164 argon ion laser was incident on the crystal which was mounted on a calibrated rotation stage. Angles in air were measured with respect to the cell faces; when the normal to the crystal face plane is parallel to the incident beam the incident angle is defined to be 90°. The angle measurements are estimated to be accurate to $\pm 0.5°$. The angles within the crystal were calculated from the measured angles in air using Snell's law. A circular aperture before the crystal defined the incident beam diameter to be 2.6 ± 0.1 mm, and neutral density filters limited the inci-

[a] Materials Science Division, Indira Gandhi Centre for Atomic Research, Kalpakkam, 603102, India.
[b] Author to whom correspondence should be addressed.

 0021-9606/91/141249-09$03.00

dent beam intensity to $3.0 \pm 0.1\ \mu W/cm^2$. These low incident intensities were necessary to avoid local crystal compression due to temperature increases in the illuminated region.[13]

The diffracted intensity was measured as a function of the angle of incidence in air. The diffracted light passed through a circular aperture placed 156 ($\pm$ 3) mm from the center of the crystal. This aperture defined the acceptance cone of the detected light. The light passing through the aperture was then focussed onto a 1 mm diam optic fiber using a condensing lens, and detected by a Hamamatsu S1226-18BQ photodiode coupled to the fiber optic. The incident and transmitted intensities were measured by swinging the arm holding the detector to a 0° scattering angle. The incident intensity was measured with the crystal removed, and the transmitted intensity was measured with the crystal face oriented normal to the incident beam direction. The values for the transmittance calculated from these measurements are labeled by T_{90}.

The diffracted intensity as a function of incident angle was measured for both the dyed and the undyed crystals with detector aperture openings of 2.6, 8, and 28.6 mm ($\pm$ 0.1 mm) diam. In addition, the diffracted intensity as a function of aperture diameter was measured at fixed incident angle (equal to the angle of maximum diffraction) for the dyed and undyed crystals. All intensity measurements were corrected for reflection losses and were normalized to the incident intensity.

RESULTS

The transmittances at normal incidence (T_{90}) for 514.5 nm incident light for the undyed and the dyed crystals, are 0.65 and 0.19 ($\pm$ 2%), respectively. Since neither polystyrene nor water absorb appreciably at this wavelength, and since the angle of incidence (90°) is far from the diffraction angle, the attenuation of the undyed crystal must derive from scattering from crystal defects and multiple scattering by the particles themselves. The absorption of light by the dyed crystal results in the decreased transmittance of 0.19. These transmittances correspond to linear extinction coefficients, μ_e, of 8.6 and 33.2 cm^{-1} for the undyed and the dyed crystals, respectively. Assuming similar defect densities in the two crystals the extinction coefficient increase derives from absorption by the dye.

Figure 1 shows the diffracted intensity as a function of the incident angle in air for both crystals for three detector apertures. The angular difference in peak position between the dyed and the undyed crystals results from a slight difference in particle concentration. The diffracted intensity at all angles increases with increasing aperture diameter for both crystals. However, the intensity increase is asymmetric about the diffraction peak, the increase being greater on the higher angle side. The angle of the maximum diffracted intensity increases with the aperture diameter increase.

The diffracted intensity as a function of the detector aperture diameter was measured for both the dyed and the undyed crystals with the cells fixed at the angle of maximum diffraction (Fig. 2). The diffracted intensity increases with

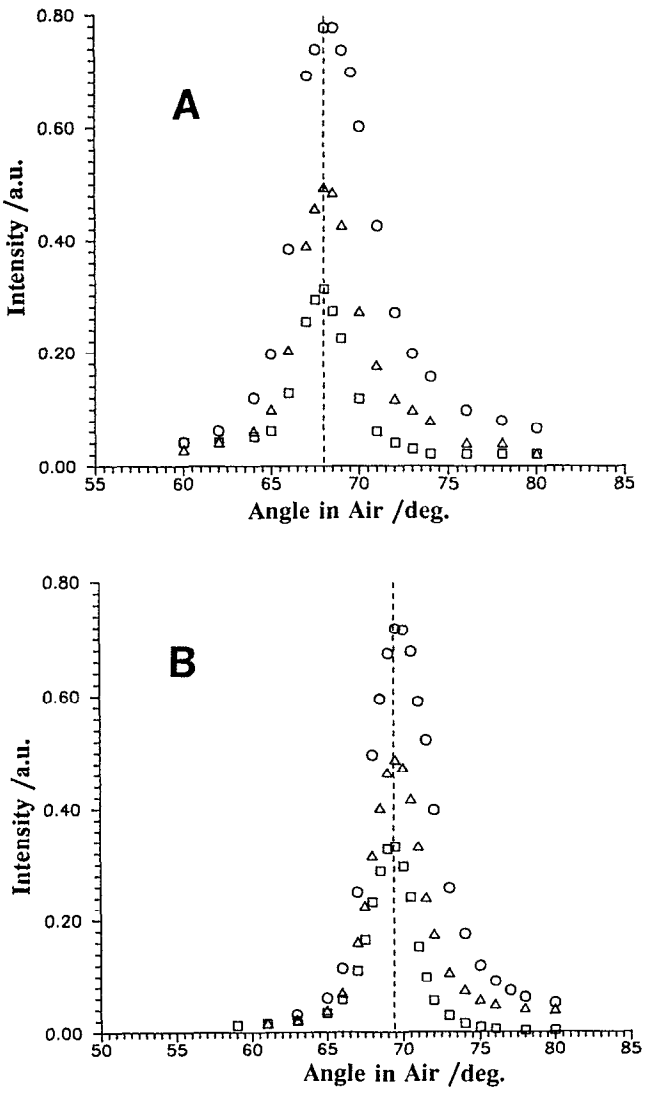

FIG. 1. Diffracted intensity as a function of the angle of incidence (in air) with detector aperture diameters of 2.6 mm (squares), 8 mm (triangles), and 28.6 mm (circles), respectively: (A) undyed crystal, (B) dyed crystal. The dashed lines denote the angle of maximum diffraction for the 2.6 mm data. The detector was placed at a scattering angle centered about the diffraction maximum.

increasing aperture diameter, which corresponds to an increasing solid angle of acceptance for the diffracted light. The intensity is close to maximum for an aperture diameter of ca. 12 mm. The total intensity increases twofold for both crystals for a collection solid angle increase from 2.2×10^{-4} to 2.6×10^{-2} sr.

DISCUSSION

The dynamical diffraction model used to quantitatively predict diffraction by nonabsorbing colloidal crystals has been presented previously.[5,15] A more general model for absorbing crystals will be presented here. For this discussion, and for the discussion of the thermal diffuse scattering, we follow the formalism of Zachariasen,[16] but appropriately

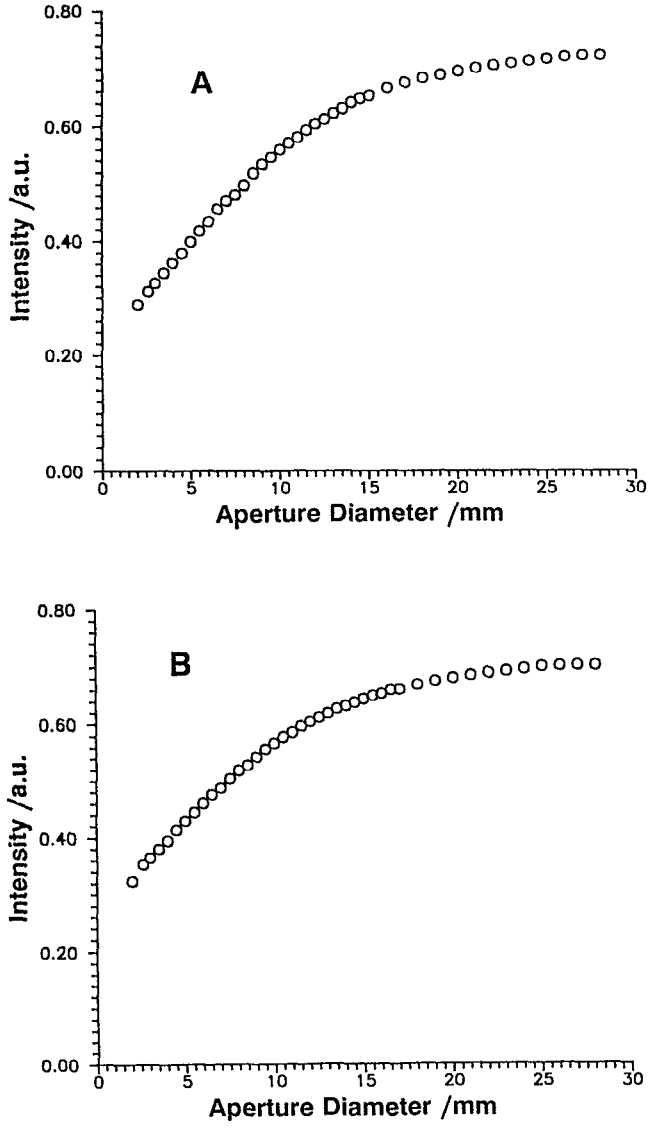

FIG. 2. Diffracted intensity as a function of aperture diameter. The crystals are fixed at the angle of maximum diffraction: (A) undyed crystal, $\theta_{\text{air}}^{m} = 68°$, (B) dyed crystal, $\theta_{\text{air}}^{m} = 69.5°$.

modify the theory to apply to colloidal crystals.

In atomic and molecular crystals the dielectric constant $\epsilon(\mathbf{r})$ is related to the polarizability per unit volume, $\alpha_0(\mathbf{r})$, by[16]

$$\epsilon(\mathbf{r}) \simeq 1 + 4\pi\cdot\alpha_0(\mathbf{r}). \tag{1}$$

For colloidal crystals, however, the dielectric constant of the surrounding medium is not unity. Consequently, we define the polarizability per unit volume of the colloidal crystal as the fractional change in the dielectric constant compared to the medium dielectric constant,

$$\frac{\epsilon(\mathbf{r})}{\epsilon_{\text{water}}} \simeq 1 + 4\pi\cdot\alpha_0(\mathbf{r}). \tag{2}$$

The three-dimensional polarizability per unit volume, $\alpha_0(\mathbf{r})$, can be expanded in a Fourier series in terms of the reciprocal lattice vectors $\mathbf{B}_H$,

$$4\pi\alpha_0(\mathbf{r}) = \psi(\mathbf{r}) = \sum_H \psi_H \cdot e^{-i2\pi\mathbf{B}_H\cdot\mathbf{r}} \tag{3}$$

where the Fourier coefficients Ψ_H are given by

$$\psi_H = \frac{1}{V_{\text{cell}}}\int_{V_{\text{cell}}} \psi(\mathbf{r}) e^{i2\pi\mathbf{B}_H\cdot\mathbf{r}} dv \tag{4}$$

and V_{cell} is the unit cell volume. $\alpha_0(\mathbf{r})$ and ψ_H are complex and we will denote the real parts with single primes and the imaginary parts with double primes, respectively. In addition, we will use the subscripts "xtl" and "air" to denote parameters within the crystal and in air, respectively. The superscripts "m" and "B" will be used to denote the parameter at the maximum and at the Bragg condition, respectively.

In the thick crystal limit, the ratio of the diffracted intensity I_D to the incident intensity I_0 is given by[16]

$$\frac{I_D}{I_0} = L - \sqrt{L^2 - (1 + 4\kappa^2)}, \tag{5}$$

where

$$L = |\sqrt{(y^2 - g_D^2 - 1)^2 + 4(g_D y - \kappa)^2}| + y^2 + g_D^2 \tag{6}$$

and

$$y = \frac{(1-b)\psi_0' + b\zeta}{2\sqrt{|b|}K|\psi_H'|}. \tag{7}$$

The unitless parameter y is determined from the angle of incidence and the diffraction peak is centered about $y = 0$. K depends upon the incident light polarization and is equal to unity for the vertically polarized incident light used in this study. The parameter b is -1 for Bragg reflections, and

$$\zeta = 2\cdot(\theta_{\text{xtl}}^{B} - \theta_{\text{xtl}})\cdot\sin(2\theta_{\text{xtl}}^{B}) \tag{8}$$

is a measure of the angular mismatch between the angle of incidence and the Bragg angle. ψ_H' is the real part of the Fourier component of the crystal polarizability with the periodicity defined by $\mathbf{B}_H$, the reciprocal lattice wavevector for the set of planes H, represented by the Miller indices $\{h,k,l\}$. Consistent with the approximation of Eq. (2), the polarizability of a dielectric sphere α_s, which is given by[17]

$$\alpha_s = \frac{1}{4\pi}\cdot(m_i^2 - 1)\cdot V_{\text{sphere}} \tag{9}$$

is substituted for the polarizability of an electron. ψ_H' is then given by

$$\psi_H' = (m_i^2 - 1)\cdot\frac{V_{\text{sphere}}}{V_{\text{cell}}}\cdot 2\cdot G(u), \tag{10}$$

where m_i is the ratio of the refractive index of the sphere to that of the medium, and V_{sphere} is the sphere volume. The structure factor F_H of a body-centered-cubic colloidal crystal is $2\cdot G(u)$.[5,15] $G(u)$ is the scattering factor per sphere,[15,16] which in the Rayleigh–Gans limit is[17]

$$f = G(u) = (3/u^3)[\sin(u) - u\cdot\cos(u)], \tag{11}$$

where $u = (4\pi n_s a/\lambda_0)\sin\theta_{\text{xtl}}^{B}$, and n_s is the suspension refractive index for λ_0, the incident wavelength as measured in air. a is the sphere radius.

The quantity g_D measures the attenuation of the inci-

dent beam due to scattering and absorption, and is given by

$$g_D = \frac{(1-b)\psi_0''}{2\sqrt{|b|}K|\psi_H'|}, \tag{12}$$

where ψ_0'' is related to the measured linear extinction coefficient by

$$\mu_e = \frac{2\pi n_s}{\lambda_0}\cdot\psi_0''. \tag{13}$$

ψ_0'' is the imaginary part of the average crystal polarizability, and ψ_0' is the real part of the average crystal polarizability.

The Fourier components ψ_H also have imaginary parts, and the parameter κ is defined by the ratio of the imaginary to the real part, $\kappa = \psi_H''/\psi_H'$.[16] κ is equal to zero (i.e., ψ_H'' is equal to zero) for the nonabsorbing (undyed) colloidal crystal since scattering from random crystal defects will not, in general, have the periodicity of the lattice. Our previous studies of diffraction were in the limit of κ equal to zero.[5]

The absorbing colloidal crystal has dye embedded in the spheres which attenuates the incident light and κ will not be zero. We estimate the upper limit for ψ_H'' for the absorbing crystal used in this study, and hence κ, by assuming that all of the dye in the crystal is spread in slabs 83 nm thick, equal to the particle diameter, and separated by 198 nm, the interplaner spacing of the bcc (110) planes. Then ψ_H'' is very approximately given by

$$\psi_H'' \simeq \frac{\lambda_0}{2\pi n_s}\cdot\mu_d\cdot\frac{198}{83} = 3.6\times10^{-4}, \tag{14}$$

where μ_d is the difference between the measured extinction coefficients μ_e for the dyed and the undyed crystals.[18]

We determined the dynamical parameter ψ_0' experimentally by measuring the wavelength of minimum transmission as a function of the angle of incidence and by fitting the data to the dynamical diffraction equation[16]

$$\lambda_{\text{xtl}}^{m} = 2n_s d_{hkl}\cdot\sin(\theta_{\text{xtl}}^{m})\cdot\left[1-\frac{1-b}{4b\cdot\sin^2(\theta_{\text{xtl}}^{m})}\cdot\psi_0'\right], \tag{15}$$

where λ_{xtl}^{m} is the wavelength of maximum diffraction at the incident angle θ_{xtl}^{m}, and d_{hkl} is the interplanar spacing for the set of diffraction planes of Miller indices $\{hkl\}$. Figure 3 shows plots of the dynamical parameter ψ_0' as a function of the incidence angle in air for the dyed and the undyed colloidal crystals.

Assuming that the primary mechanism responsible for decreasing the diffracted intensity, at least for the nonabsorbing crystal, is inelastic scattering from crystal phonon modes, the measured ratio I_D/I_0 is given by[19]

$$\left(\frac{I_D}{I_0}\right)_{\text{total}} = \left(\frac{I_D}{I_0}\right)_{\text{ideal}}\cdot e^{-2M} + \frac{J_2}{I_0}, \tag{16}$$

where $(I_D/I_0)_{\text{ideal}}$ refers to the ratio given by Eq. (5) with a value for g_D which was calculated from the experimentally determined linear extinction coefficient using Eqs. (12) and (13), and e^{-2M} is the Debye–Waller factor. The product $(I_D/I_0)_{\text{ideal}}\cdot e^{-2M}$ is the zero-phonon contribution to the measured diffracted intensity. The factor J_2/I_0 represents the contribution to the diffracted intensity due to scattering from all crystal phonons. The measured intensity represents the light diffracted from instantaneous crystal structures averaged over the time of the measurement.

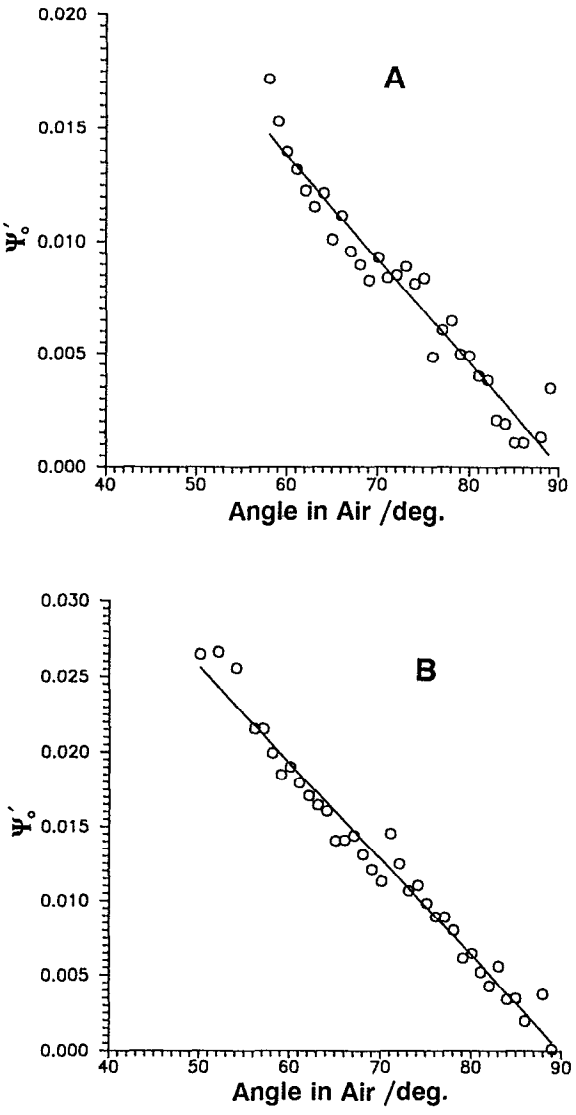

FIG. 3. The dynamical parameter ψ_0' as a function of the angle of maximum diffraction: (A) undyed crystal, (B) dyed crystal.

The first term of Eq. (16), which represents the coherent part of the scattered light, is interpreted as light diffracted from the mean crystal lattice. The Debye–Waller factor[19] e^{-2M} is obtained by fitting the first term of Eq. (16) [i.e., Eq. (5)] to the diffraction data for a detector aperture diameter of 2.6 mm. This aperture opening, which is equal to the incident beam diameter, limits the collected intensity to mainly zero-phonon scattered light. Figure 4 shows the fits for the dyed and undyed crystals, and Table I lists the parameters used in the calculation. This figure shows that absorption by the dye skews the diffraction band shape, especially near the maximum. However, the postion of the peak center is essentially independent of κ for the range of absorption values used in this study.

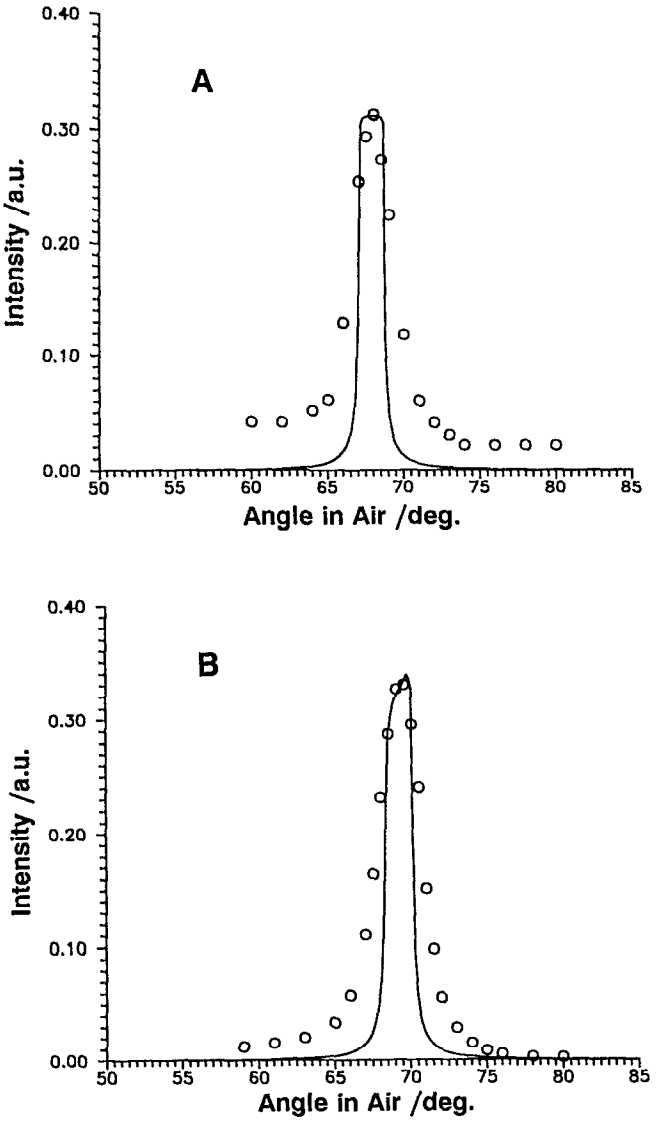

FIG. 4. Calculated diffraction peaks and the experimental data points for the 2.6 mm aperture. The Debye–Waller factor e^{-2M} was determined by fitting the calculated maximum diffraction intensity to the data. (A) Undyed crystal, (B) dyed crystal.

TABLE I. Parameters used to calculate the diffraction peaks in the dynamical diffraction limit.

	Undyed	Dyed
n_s (at 514.5 nm)	1.3415	1.3424
d_{hkl} (nm)	199.2	198.0
T_{90}	0.65	0.19
μ_e (cm^{-1})	8.6	33.2
e^{-2M}	0.315	0.34
θ^B_{xtl} (rad)	1.2964	1.3172
n_p (cm^{-3})	8.92×10^{13}	9.09×10^{13}
Ψ''_0	5.24×10^{-5}	2.00×10^{-4}
Ψ''_H	0.0	3.6×10^{-4}
Ψ'_H	9.90×10^{-3}	1.01×10^{-2}
v_0 (cm/s)	93.08	93.11

The second term in Eq. (16) is the incoherent part of the scattering due to thermally induced lattice vibrations. Following the lead of Zachariasen,[19] we adopt the Debye approximation to account for light scattered by phonons which assumes that all phonon branches follow the linear dispersion relation given by

$$\omega = v_0 \cdot q, \tag{17}$$

where v_0 is the phonon propagation velocity and q is the phonon wave vector. Substituting the dielectric sphere polarizability for the dipole moment of an electron induced by unit field, we arrive at the following expression for J_2/I_0 at an angle of incidence equal to the angle of maximum diffraction for a wave vector q (see Appendix)

$$\left(\frac{J_2}{I_0}\right)_q = \frac{64\pi^4 n_s^6 \alpha_s^2}{m\lambda_0^6 R^2} n_p A \left(\frac{1-e^{-2\mu t_0}}{2\mu}\right) \times f^2 e^{-2M} \cdot \sin^2(\theta^m_{\text{xtl}}) \cdot \frac{4\pi^2 Q}{v_0^2 q^2}, \tag{18}$$

where n_p is the particle number density, A is the incident beam cross section, R is the distance from the crystal to the detector aperture, m is the mass of a sphere. The effective scattering volume V_{scat} is calculated by averaging over the intensity as a function of crystal penetration depth [see Eq. (24)],

$$V_{\text{scat}} = A\left(\frac{1-e^{-2\mu t_0}}{2\mu}\right), \tag{19}$$

where μ is the extinction coefficient (see below) and t_0 is the total path length of the light in the crystal. The mean energy Q for a phonon of frequency ω is found from[19]

$$Q = \frac{(h/2\pi)\omega}{e^{(h\omega/2\pi k_b T)} - 1} + \frac{h}{4\pi}\omega \simeq k_b T + \frac{h\omega}{4\pi} \tag{20}$$

for small ω where h is Planck's constant and k_b is the Boltzmann constant.

The total extinction coefficient μ is given by the sum of the extinction coefficients due to Bragg diffraction μ_B, linear absorption μ_A, and scattering from crystal defects μ_s,

$$\mu = \mu_B + \mu_A + \mu_S \tag{21}$$

and t_0 is given by $L/\sin\theta_{\text{xtl}}$, where L is the crystal thickness. The experimentally determined transmittance away from the Bragg condition gives the contributions to μ due to absorption and scattering from defects. The extinction due to Bragg diffraction μ_B, however, is not known.

The experimental scattered intensities as a function of phonon wave vector were determined from the data shown in Fig. 2 using the geometry illustrated in Fig. 5. The relative intensity differences between aperture diameters were calculated to yield the integrated intensity within annular regions defined by circles of radii r_1 and r_2, of an average radius r_m. At radius r, the magnitude of the phonon wave vector is

$$q \cong \frac{2\pi}{\lambda_0}\frac{r}{R}, \tag{22}$$

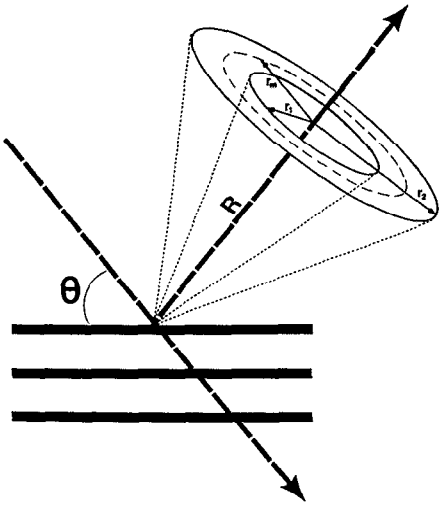

FIG. 5. Geometry for measuring TDS intensity as a function of phonon wave vector q. The diffracted intensity collected with an aperture radius r_1 is subtracted from the intensity collected with radius $r_2 > r_1$. The resultant intensity difference corresponds to the total intensity of the annular region between r_1 and r_2, and is associated with the phonon wave vector q calculated from the mean radius of the annulus r_m, using Eq. (22).

where R is the distance from the crystal to the aperture.

The measured intensity contains thermal diffuse scattering (TDS) contributed by phonons with wavevectors from q_1 to q_2 (defined by aperture radii r_1 and r_2) as shown in Fig. 6. The sum of the incident wave vector $\mathbf{k}_0$ and the reciprocal lattice vector $\mathbf{B}_H$ gives the Bragg diffracted wave vector $\mathbf{k}_{s,0}$. The phonon with wave vector of $\mathbf{q}_2$ scatters the Bragg diffracted wave into the TDS scattered wave with wave vector $\mathbf{k}_{s,2}$, which also lies on the sphere of reflection.

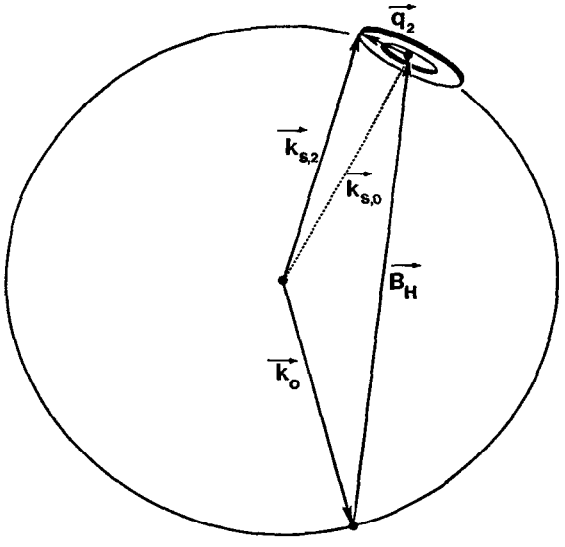

FIG. 6. Schematic reciprocal space representation of the thermal diffuse scattering measurements. The colloidal crystal is fixed at the angle of maximum diffraction. The diffusely scattered intensity about the Bragg direction (defined by $\mathbf{k}_{s,0}$) derives from phonons of wave vector $\mathbf{q}$.

Since we measure all of the scattered intensity between aperture radii r_1 and r_2, the expression for J_2/I_0 given in Eq. (18) must be integrated over phonon wave vectors from $\mathbf{q}_1$ to $\mathbf{q}_2$. The number of phonons contributing to the measured TDS intensity is[20]

$$\frac{V_{\rm ill}}{(2\pi)^3}\int_{q_1}^{q_2} 2\pi q\, dq\cdot\frac{2\pi}{(V_{\rm ill})^{1/3}}, \tag{23}$$

where $2\pi/(V_{\rm ill})^{1/3}$ is the shortest reciprocal lattice spacing between phonon wave vectors, $2\pi q\, dq$ is the detection annular area in reciprocal space, and $V_{\rm ill}$ is the illuminated volume, which can be obtained from

$$V_{\rm ill} = \int_0^{t_0} Ae^{-\mu t}\, dt = \frac{A(1-e^{-\mu t_0})}{\mu}. \tag{24}$$

We calculate the phonon density based on the illuminated volume rather than the total crystal volume since the phonons in general are overdamped in colloidal crystals.[21,22] Those phonons, however, known not to be heavily overdamped in colloidal crystals,[12,23] have frequencies smaller ($< 10^4$ Hz) than those examined in this study ($> 10^5$ Hz). Therefore, the assumption of overdamped phonons, and limiting the particles involved to the illuminated volume, is appropriate here.

The diffusely scattered intensity passing through the annular region defined by r_1 and r_2 can then be written

$$\left(\frac{J_2}{I_0}\right)_{q_1\to q_2} = \frac{(V_{\rm ill})^{2/3}}{2\pi}\int_{q_1}^{q_2} q\left(\frac{J_2}{I_0}\right)_q dq. \tag{25}$$

Substituting Eqs. (20), (23), and (24) into Eq. (25), and integrating over q, gives

$$\begin{aligned}\left(\frac{J_2}{I_0}\right)_{q_1\to q_2} &= \frac{64\pi^4 n_s^6\alpha_s^2}{m\lambda_0^6 R^2}\cdot n_p\cdot f^2\cdot e^{-2M}\cdot\sin^2\theta^m_{\rm xtl}\\ &\quad\cdot A\cdot\frac{1-e^{-2\mu t_0}}{2\mu}\cdot\left(A\cdot\frac{1-e^{-\mu t_0}}{\mu}\right)^{2/3}\\ &\quad\cdot\left[\frac{2\pi k_b T}{v_0^2}\ln\left(\frac{q_2}{q_1}\right)+\frac{h}{2v_0}(q_2-q_1)\right]\end{aligned} \tag{26}$$

for the diffuse scattered intensity resulting from phonons of magnitude between q_1 and q_2.

The extinction coefficient due to Bragg scattering μ_B is used as a fitting parameter in Eq. (26). The average phonon velocity v_0 is calculated from the crystal elastic modulus, which is given by[21]

$$E = B + \tfrac{4}{3}C. \tag{27}$$

The crystal bulk modulus B and shear modulus C are found from the interparticle interaction potential $U(d)$ and for a bcc crystal are given by[24]

$$B = \tfrac{4}{9}\cdot n_p\cdot(\kappa d+2)^2\cdot U(d) \tag{28}$$

and

$$C = \tfrac{4}{5}\cdot n_p\cdot(\kappa d)^2\cdot U(d). \tag{29}$$

The screened Coulomb interparticle interaction potential $U(d)$ is given by[25]

$$U(d) = \frac{Z^2e^2}{\epsilon}\cdot\frac{e^{2\kappa a}}{(1+\kappa a)^2}\cdot\frac{e^{-\kappa d}}{d}, \tag{30}$$

where Z is the effective number of surface charges per sphere, taken to be the renormalized charge[26] of 1150, e is the electronic charge, ϵ is the suspension dielectric constant (taken to be that of water), a is the sphere radius, and d is the interparticle separation distance. The inverse Debye screening length κ is defined by

$$\kappa^2 = \frac{4\pi e^2}{\epsilon k_b T} \cdot (n_p Z + n_i), \tag{31}$$

where n_i is the ionic impurity concentration (unknown). As in our previous work,[13] we will assume that n_i is equal to $n_p Z$. We justify this assumption based on the previous studies of Lindsay and Chaikin,[27] and Kesavamoorthy.[28] Lindsay and Chaikin[27] measured the shear moduli as a function of added HCl for colloidal crystals consisting of 109 nm diam spheres, with 600 surface charge groups per sphere (determined by conductometric titration). The measured shear moduli could only be rationalized using a screened Coulombic interaction potential if the number of surface charge groups is decreased to 305 if no ionic impurities were present in the colloidal suspensions prior to addition of HCl.[27] This was not a physically reasonable result; little or no charge renormalization is required at the value of Z of 600 charges/sphere.[26] Kesavamoorthy found that Lindsay and Chaikin's elastic constant data could be equally rationalized for the measured sphere charge if the ionic impurity concentration n_i prior to addition of HCl were set equal to $n_p Z$.[28] Thus, we assume an impurity concentration for our colloidal crystals of $n_p Z$.

The average phonon velocity is found from the elastic modulus,[21]

$$v_0 = \sqrt{\frac{E}{m \cdot n_p}}, \tag{32}$$

where m is the mass of a sphere. The average phonon velocities calculated in this way are listed in Table I.

Figure 7 shows the data and the calculated fit using Eq. (26) with μ_B as the only fitting parameter. A best fit was obtained for the dyed crystal with $\mu_B = 500\ \text{cm}^{-1}$, and for the undyed crystal, $\mu_B = 450\ \text{cm}^{-1}$. Thus, the total extinction coefficients are 533.2 and 458.6 cm^{-1} for the dyed and the undyed crystals, respectively. Therefore, the effective penetration depths of the incident electric field when the diffraction condition is satisfied (i.e., the depth at which the incident intensity decreases by $1/e$ of its initial value) in these colloidal crystals are 19 and 22 μm for the dyed and the undyed crystals, respectively.

For an ideal crystal in the Bragg diffraction limit (i.e., no lattice vibrations), the ratio of the diffracted to the incident intensities when the incident angle equals the angle of maximum diffraction is given by[16]

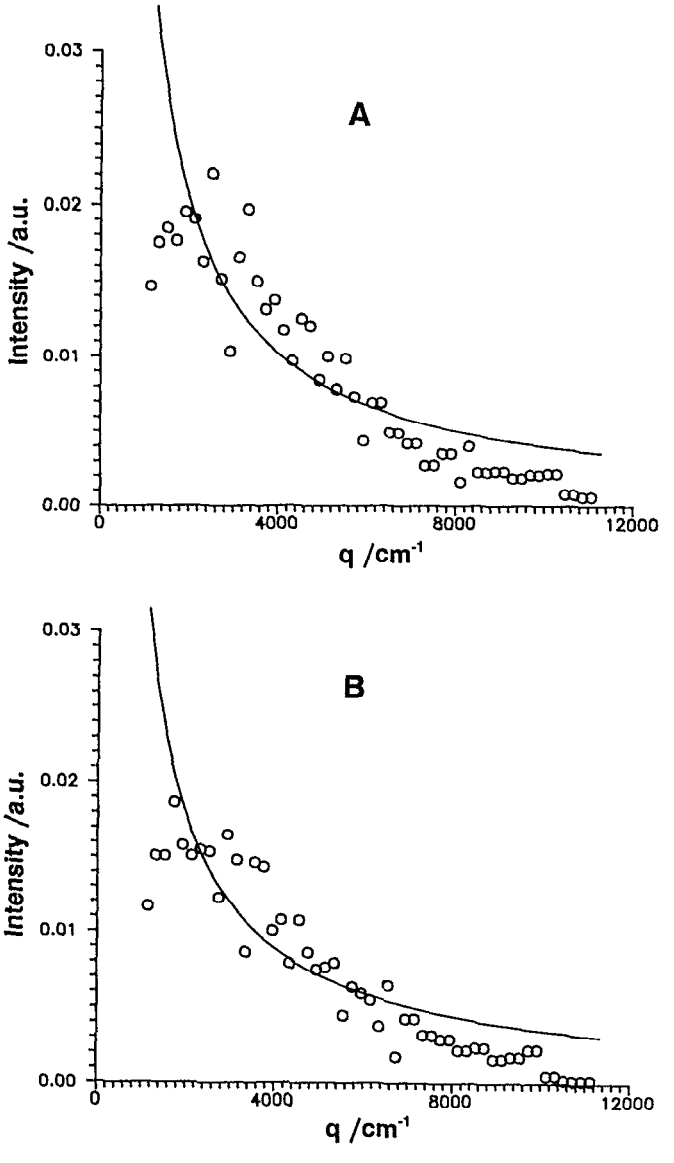

FIG. 7. Experimental TDS intensities and the theoretical fits with the Bragg extinction coefficient μ_B as the only fitting parameter: (A) undyed crystal, $\mu_B = 450\ \text{cm}^{-1}$, (B) dyed crystal, $\mu_B = 500\ \text{cm}^{-1}$.

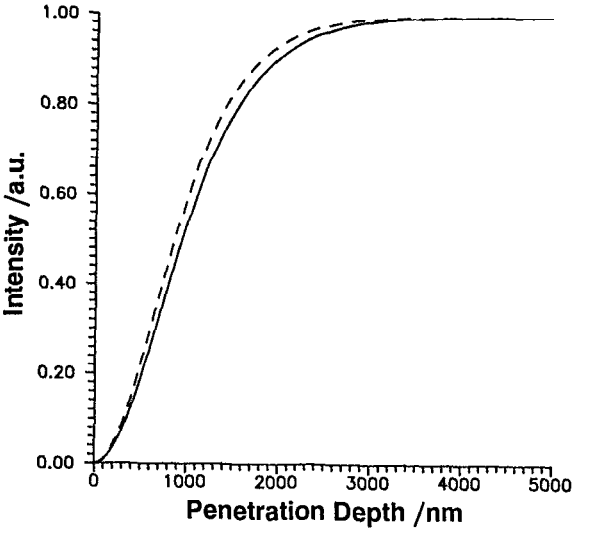

FIG. 8. Plots of I_D/I_0 as a function of the penetration depth t for the ideal crystal Bragg case calculated using Eq. (33) for the undyed crystal (solid line) and the dyed crystal (dashed line).

$$\left[\frac{I_D}{I_0}\right]_{\text{ideal}} = \frac{\sinh^2(\pi \cdot k_0 \cdot \psi'_H \cdot t)}{1 + \sinh^2(\pi \cdot k_0 \cdot \psi'_H \cdot t)}, \tag{33}$$

where $k_0 = 2\pi n_s/\lambda_0$. Figure 8 shows the plots of this ratio for the two crystals studied here as a function of the penetration depth t. All of the incident light is diffracted away within the first four microns in this ideal case, and the effective penetration depth is approximately 1 μm for both crystals. Thus, the incident light penetrates greater than 15 times farther into the real colloidal crystal than the ideal crystal due to the presence of crystal defects and thermal diffuse scattering.

In the kinematic limit, the thermal diffuse scattering intensity distribution is centered about the Bragg angle.[19] However, one of the results of the dynamical diffraction theory is that the angle of maximum diffraction does not equal the Bragg angle. We expected that the TDS intensity distribution in the dynamical diffraction limit would be centered about the angle of maximum diffraction rather than about the Bragg angle. In contrast, our experimental data suggest that the TDS scattering is centered about the Bragg angle. We subtracted the 8 mm aperture diameter diffraction data from the 28.6 mm data, and the 2.6 mm data from the 8 mm data, for both crystals. The intensity difference, which are plotted as a function of the angle of incidence in Fig. 9, are centered at angles greater than the maximum diffraction angle (delineated by the solid vertical lines) close to the Bragg angle (depicted by dashed lines in Fig. 9, calculated from the dynamical parameter ψ'_0 for colloidal crystals[5]). Table II lists the angles determined for maximum diffraction, the Bragg angle and the central angle for the TDS. The similarity between $\theta^{\text{TDS}}_{\text{air}}$ and θ^{B}_{air} suggests that the thermal diffuse scattering for colloidal crystals may be centered about the Bragg angle. We do not as yet understand this result.

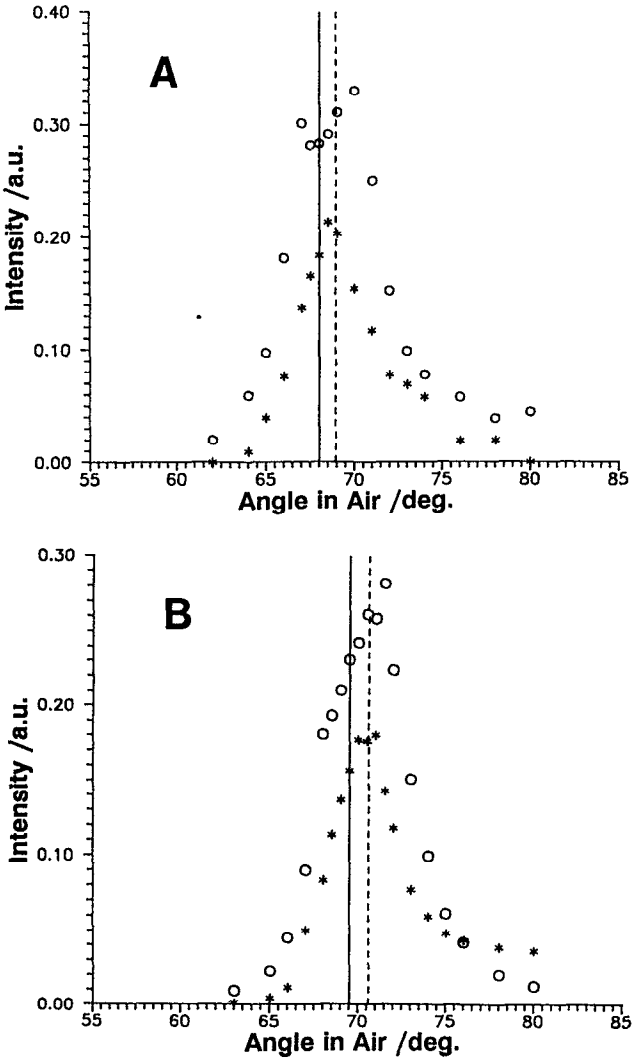

FIG. 9. Plots of the diffraction intensity differences as a function of angle (in air) between the data collected with an aperture diameter of 28.6 and 8 mm (circles), and between diameters of 8 and 2.6 mm (stars): (A) undyed crystal, (B) dyed crystal. In both cases the peak centers are at higher angles than the reported angles of maximum diffraction. The dashed lines denote the Bragg angles calculated from the ψ'_0 data of Fig. 3, and the solid lines denote the angle of maximum diffraction for the 2.6 mm aperture diameter data.

TABLE II. Angles in air of the maximum diffraction (approximately zero phonon), Bragg, and the center of the TDS distribution.

Crystal	θ^{m}_{air}	θ^{B}_{air}	$\theta^{\text{TDS}}_{\text{air}}$
Undyed	68.0°	69.0°	68.8°
Dyed	69.5°	70.6°	70.5°

SUMMARY

We show that dynamical diffraction theory accurately describes the diffraction of light from nonabsorbing and absorbing colloidal crystals. In addition, we show that the Debye treatment of crystal lattice vibrations can be used to model TDS intensity distributions about the Bragg spot for colloidal crystals, and that the effective penetration depth of the electric field can be determined from the diffuse scattering intensity distribution when the diffraction conditions are satisfied. Finally, the data suggest that the TDS intensity is distributed about the Bragg angle rather than about the angle of maximum diffraction.

APPENDIX

When the diffraction conditions are satisfied for an atomic crystal the thermal diffuse scattering (TDS) intensity deriving from a phonon of wave vector magnitude q is approximately given by Eq. (4.133) from Ref. 19,

$$\left|\frac{J_2}{I_e}\right|_q \simeq \frac{4Nf^2e^{-2M}}{m\lambda^2} \cdot \sin^2\theta^{m}_{\text{xtl}} \cdot \frac{Q \cdot 4\pi^2}{v_0^2 q^2}, \tag{A1}$$

where N is the total number of primitive unit cells in the crystal giving rise to TDS intensity ($N = n_p V_{\text{scat}}$), and I_e is related to the incident intensity by [Eq. (3.11) of Ref. 16]

$$I_e = I_0\left(\frac{e^2 \sin\phi}{mc^2R}\right)^2, \tag{A2}$$

where ϕ is the angle between the electric field vector of the incident x-ray radiation and the scattering direction (for

vertically polarized incident light $\sin\phi = 1$). For a single electron, the dipole moment induced by unit field is

$$|\alpha_e| = \frac{e^2}{m\omega^2}. \tag{A3}$$

Thus,

$$\frac{e^2}{mc^2} = \frac{e^2 4\pi^2}{m\omega^2\lambda^2} = |\alpha_e| \cdot \frac{4\pi^2}{\lambda^2}. \tag{A4}$$

To extend this theory to describe the thermal diffuse scattering of visible light by colloidal crystals we substitute the polarizability of a dielectric sphere α_s for $|\alpha_e|$, and λ_0/n_s for λ. Thus

$$I_e = I_0 \alpha_s^2 \frac{16\pi^4 n_s^4}{\lambda_0^4 R^2}, \tag{A5}$$

where it is understood that I_e now refers to the scattering of light by a sphere. Substituting Eq. (A5), and $n_p V_{\text{scat}}$ for N, into Eq. (A.1) gives

$$\left|\frac{J_2}{I_0}\right|_q \simeq \frac{64\pi^4 n_s^6 \alpha_s^2}{m\lambda_0^6 R^2} \cdot n_p \cdot V_{\text{scat}} \cdot f^2 \cdot e^{-2M} \cdot \sin^2\theta_{\text{xtl}}^m \cdot \frac{Q \cdot 4\pi^2}{v_0^2 q^2}. \tag{A6}$$

[1] P. Pieranski, Contemp. Phys. **24**, 25 (1983).
[2] N. A. Clark, A. J. Hurd, and B. J. Ackerson, Nature (London) **281**, 57 (1979).
[3] Y. Monovoukas and A. P. Gast, J. Colloid Interface Sci. **128**, 533 (1989).
[4] M. O. Robbins, K. Kremer, and G. S. Grest, J. Chem. Phys. **88**, 3286 (1988).
[5] P. A. Rundquist, P. Photinos, S. Jagannathan, and S. A. Asher, J. Chem. Phys. **91**, 4932 (1989).
[6] P. A. Hiltner and I. M. Krieger, J. Phys. Chem. **73**, 2386 (1969).
[7] R. J. Carlson and S. A. Asher, Appl. Spectrosc. **38**, 297 (1984).
[8] S. A. Asher, P. L. Flaugh, and G. Washinger, Spectroscopy **1**, 26 (1986).
[9] P. L. Flaugh, S. E. O'Donnell, and S. A. Asher, Appl. Spectrosc. **38**, 847 (1984).
[10] S. A. Asher, U. S. Patent Nos. 4,627,689 and 4,632,517.
[11] A. J. Hurd, N. A. Clark, R. C. Mockler, and W. J. O'Sullivan, Phys. Rev. A **26**, 2869 (1982).
[12] A. J. Hurd, *The Lattice Dynamics of Colloidal Crystals* (PhD. Dissr., University of Colorado, 1981).
[13] P. A. Rundquist, S. Jagannathan, R. Kesavamoorthy, C. Brnardic, S. Xu, and S. A. Asher, J. Chem. Phys. **94**, 711 (1991).
[14] D. W. Schaefer, J. Chem. Phys. **66**, 3980 (1977).
[15] R. J. Spry and D. J. Kosan, Appl. Spectrosc. **40**, 782 (1986).
[16] W. H. Zachariasen, *Theory of X-Ray Diffraction in Crystals* (Wiley, New York, 1945), Chap. 3.
[17] H. C. van de Hulst, *Light Scattering by Small Particles* (Dover, New York, 1981), Chap. 7.
[18] P. A. Gohman, G. Bambakidis, and R. J. Spry, J. Appl. Phys. **67**, 40 (1990).
[19] Ref. 16, Chap. 4.
[20] See, for instance, J. S. Blakemore, *Solid State Physics*, 2nd ed. (Cambridge, New York, 1988), Chap. 2.
[21] F. Grüner and W. P. Lehmann, J. Phys. A **15**, 2847 (1982).
[22] T. Ohtsuki, S. Mitaku, and K. Okano, Jpn. J. Appl. Phys. **17**, 627 (1978).
[23] J. F. Joanny, J. Colloid Interface Sci. **71**, 622 (1979).
[24] R. Kesavamoorthy and A. K. Arora, J. Phys. C **19**, 2833 (1986).
[25] D. Thirumalai, J. Phys. Chem. **93**, 5637 (1989).
[26] S. Alexander, P. M. Chaiken, P. Grant, G. J. Morales, P. Pincus, and D. Hone, J. Chem. Phys. **80**, 5776 (1984).
[27] H. M. Lindsay and P. M. Chaikin, J. Chem. Phys. **76**, 3774 (1982).
[28] R. Kesavamoorthy, PhD. Disser., Indira Gandhi Centre for Atomic Research, Kapakkam, India, 1987.